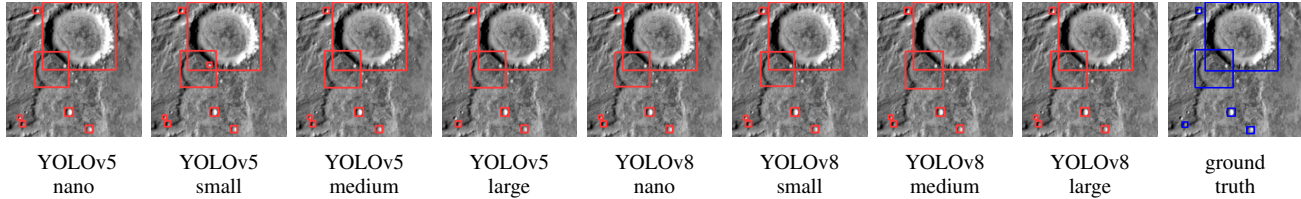


# EVALUATION OF RESOURCE-EFFICIENT CRATER DETECTORS ON EMBEDDED SYSTEMS

Simon Vellas<sup>1</sup>, Bill Psomas<sup>1</sup>, Kalliopi Karadima<sup>1</sup>, Dimitrios Danopoulos<sup>1</sup>,  
Alexandros Paterakis<sup>1</sup>, George Lentaris<sup>1</sup>, Dimitrios Soudris<sup>1</sup>, Konstantinos Karantzas<sup>1</sup>

<sup>1</sup>National Technical University of Athens



**Figure 1:** Qualitative comparison of crater detection results of YOLOv5 [1] and YOLOv8 [2] on a Mars image [3]. Visualizations show the predicted bounding boxes across different model sizes. The final column shows the ground truth for reference.

## ABSTRACT

Real-time analysis of Martian craters is crucial for mission-critical operations, including safe landings and geological exploration. This work leverages the latest breakthroughs for on-the-edge crater detection aboard spacecraft. We rigorously benchmark several YOLO networks using a Mars craters dataset, analyzing their performance on embedded systems with a focus on optimization for low-power devices. We optimize this process for a new wave of cost-effective, commercial-off-the-shelf-based smaller satellites. Implementations on diverse platforms, including Google Coral Edge TPU, AMD Versal SoC VCK190, Nvidia Jetson Nano and Jetson AGX Orin, undergo a detailed trade-off analysis. Our findings identify optimal network-device pairings, enhancing the feasibility of crater detection on resource-constrained hardware and setting a new precedent for efficient and resilient extraterrestrial imaging. Code at: [https://github.com/billpsomas/mars\\_crater\\_detection](https://github.com/billpsomas/mars_crater_detection).

**Index Terms**— Object Detection, Edge Computing, Mars

## 1. INTRODUCTION

Impact craters are prevalent across the solar system, including planets, moons, asteroids, transneptunian objects, and occasionally comets [4]. They form from meteoroid, asteroid, or comet impacts [5, 6], and are critical for understanding geomorphological processes [7].

Crater studies offer insights into the early evolution of solar system bodies, such as moons orbiting planets [8, 9]. They help determine the ages of planetary bodies [10, 11, 12, 13], study material deposition, and explore climatic history and potential habitability [14, 15, 16, 17, 18, 19].

Crater detection is vital for autonomous navigation and landing in space missions. Despite advances in deep learning,

there is a lack of thorough evaluation for *real-world, onboard space applications*. Automated crater detection can improve navigation accuracy and safety in space missions [20], particularly for autonomous probes and landers [21, 22, 23].

Initially, crater detection relied on *manual inspection* by experts, resulting in extensive crater databases for Mars and the Moon [24, 25, 26]. This approach was time-consuming, labor-intensive, and prone to variability [27], leading to the development of automated *crater detection algorithms* utilizing features like shape, edge, and contour [28, 29, 30, 31, 32, 33]. However, these algorithms faced challenges in large-scale and diverse diameter range detection [34, 35, 36, 37].

Deep learning has enabled more accurate and efficient crater detection [38, 39, 40]. Deploying these algorithms in space missions poses challenges regarding *reliability* in harsh environments. CMOS technologies are prone to space-induced errors, necessitating *fault-tolerant* techniques for commercial off-the-shelf processors and cameras. Issues like transient bit-flips in SRAM-based FPGAs or accumulated dose effects on camera sensors can impact performance [41, 42]. Thus, optimizing networks for embedded systems and enhancing their *resilience* against radiation effects through software mitigation is crucial.

This work focuses on training YOLO [43, 44, 2] networks for real-time crater detection (Figure 1). YOLO’s object detection capabilities and efficiency make it suitable for planetary exploration missions. Evaluating these networks on embedded systems and conducting network/device *pair exploration* and *trade-off analysis* aims to improve resilient deep learning solutions in orbit.

In summary, we make the following contributions:

1. We train several efficient crater detection networks on a publicly available benchmark dataset.

2. We evaluate these networks on several embedded processing systems.
3. We conduct a network/device pair exploration and trade-off analysis.

## 2. RELATED WORK

**Crater Detection:** Methodologies have evolved from *manual inspection* by experts to *automated algorithms* and, more recently, *deep learning*. Initially, planetary geologists manually inspected high-resolution images to identify and catalog craters [45]. This method, though foundational, was limited by *subjective interpretation* and lacked scalability.

Automated *crater detection algorithms* (CDA) emerged to address these challenges. Techniques include the combinational Hough transform [46], continuously scalable template matching (CSTM) [47], shape recognition [48], and processing highlight and shadow features using inverted images [49].

Detecting craters at large scales and across diverse diameters is challenging, but some studies have addressed these for global surveys [50]. Deep learning has further enhanced crater detection by allowing algorithms to develop their own features, improving efficiency and accuracy [51, 38, 39, ?]. Recent methods utilize convolutional neural networks to automatically learn and extract features, significantly advancing the field.

**Benchmarking:** Accurate *benchmarking* of processing architectures ensures they meet the *computational demands* of modern edge applications, such as data processing, scientific measurements, autonomous navigation, and real-time decision-making. Simulating operational environments and stress-testing capabilities help identify potential failures and *optimize* configurations. Due to constant advancements, reviewing the state-of-the-art in embedded computing is essential [52]. The rapid growth of AI necessitates low-latency, efficient data processing close to the source [53, 54].

Machine learning algorithms on spacecraft are critical for autonomous navigation and landing. The rise of commercially available embedded devices that address increased processing needs while maintaining low power consumption has garnered significant interest in the space community [55]. This interest is evident in mission-specific applications such as earth observation, remote sensing [56], and spacecraft pose estimation [57].

## 3. PROBLEM FORMULATION

Given an image  $X \in \mathbb{R}^{H \times W \times C}$ , where  $H$  is the height,  $W$  is the width, and  $C = 1$  for grayscale images, the task is to detect craters. The goal is to train an object detection model  $f$ , parameterized by  $\theta$ , that predicts bounding boxes and confidence scores for craters:

$$\hat{y} = f(X; \theta) \quad (1)$$

The predictions  $\hat{y}$  include bounding boxes  $B$  and confidence scores  $S$ :

$$\hat{y} = \{(B_i, S_i) \mid i = 1, \dots, N\},$$

where  $N$  is the number of predictions. Each  $B_i$  is represented by  $(x_i, y_i, w_i, h_i)$ , with  $(x_i, y_i)$  as the center and  $w_i, h_i$  as the width and height. The confidence score  $S_i \in [0, 1]$  indicates the likelihood of a crater.

Let  $y$  be the ground truth annotations:

$$y = \{B_j^{gt} \mid j = 1, \dots, M\},$$

where  $M$  is the number of ground truth bounding boxes. The loss function  $L$  used to train  $f$  consists of localization loss  $L_{loc}$  and confidence loss  $L_{conf}$ . The total loss  $L$  is:

$$L = \alpha L_{loc} + \beta L_{conf} \quad (2)$$

The training objective is to find the optimal parameters  $\theta^*$  that minimize  $L$ :

$$\theta^* = \arg \min_{\theta} L(f(X; \theta), y) \quad (3)$$

By optimizing this, the model  $f$  learns to detect craters accurately, providing bounding boxes and confidence scores.

## 4. EXPERIMENTS

### 4.1. Models

We use YOLOv5 [1] and YOLOv8 [2]. YOLOv5 [1], developed by ultralytics [58], is an object detection model designed for real-time applications. Key features include: Cross stage partial network (CSPNet) [59] backbone, Spatial pyramid pooling (SPP) [60] layer, Path aggregation network (PANet) [61] head. YOLOv8 [2], developed by ultralytics too, introduces further optimizations for enhanced performance and accuracy: anchor-free detection, efficient convolutional design and online image augmentation.

### 4.2. Devices

We adapt and deploy models on the following embedded devices, suitable for on-board data processing in space:

- NVIDIA Jetson Nano 4GB [62]
- NVIDIA Jetson AGX Orin 64GB development kit [63]
- Google Coral Edge TPU 1GB development kit [64]
- AMD Versal SoC VCK190 evaluation kit [65]

For reference, we also include:

- ARM64 Cortex A78AE CPU [63]
- x86 Intel Xeon Gold 5218R CPU [66]
- NVIDIA V100 Tensor Core GPU [67]

DEVICE	POWER CONSUMPTION	ACCURACY & LATENCY	YOLO v5 [1]				YOLO v8 [2]			
			NANO	SMALL	MEDIUM	LARGE	NANO	SMALL	MEDIUM	LARGE
Intel Xeon x86 CPU (1-core)	100W	AP <sub>30-60</sub>	79.6	78.0	80.8	81.2	77.9	77.7	80.7	81.9
		AP <sub>50</sub>	80.2	78.0	81.4	80.9	78.9	78.3	80.1	82.5
		AR <sub>50</sub>	89.3	85.8	89.6	88.6	86.3	86.5	88.9	91.0
		$t$ (msec):	30	72	175	340	33.0	82	204	397
NVIDIA V100 Tensor Core GPU <sup>1</sup>	300W	AP <sub>30-60</sub>	79.8	77.7	80.8	81.0	77.9	77.7	80.9	81.9
		AP <sub>50</sub>	80.3	77.8	81.4	80.8	78.9	78.3	80.2	82.5
		AR <sub>50</sub>	89.4	85.8	89.6	88.5	86.3	86.3	89.0	91.0
		$t$ (msec):	1.2	1.5	2.3	3.1	1.3	1.6	2.5	3.3
ARM64 Cortex-A CPU (4-cores)	5-15W	AP <sub>30-60</sub>	79.6	78.0	80.8	81.2	77.9	77.7	80.7	81.9
		AP <sub>50</sub>	80.2	78.0	81.4	80.9	78.9	78.3	80.1	82.5
		AR <sub>50</sub>	89.3	85.8	89.6	88.6	86.3	86.5	88.9	91.0
		$t$ (msec):	104.3	214.5	478.5	850.3	114.8	246.9	538.4	990.1
Google Coral edge TPU 1GB (INT8)	5W	AP <sub>30-60</sub>	72.5	73.5	73.7	75.4	70.3	73.2	77.8	77.2
		AP <sub>50</sub>	72.4	74.8	73.4	76.2	70.1	72.9	77.8	78.5
		AR <sub>50</sub>	82.1	82.6	83.5	84.2	78.0	81.4	87.9	87.9
		$t$ (msec):	17.3	26.3	69.5	135.6	18.3	32.7	73.5	124.1
NVIDIA Jetson Nano 4GB	10W	AP <sub>30-60</sub>	79.6	78.0	80.8	81.2	77.9	77.7	80.7	81.9
		AP <sub>50</sub>	80.2	78.0	81.4	80.9	78.9	78.3	80.1	82.5
		AR <sub>50</sub>	89.3	85.8	89.6	88.6	86.3	86.5	88.9	91.0
		$t$ (msec):	24.0	35.2	75.5	151.0	25.7	40.5	79.4	159.1
NVIDIA Jetson AGX Orin 64GB	15W mode	AP <sub>30-60</sub>	79.6	78.0	80.8	81.2	77.9	77.7	80.7	81.9
		AP <sub>50</sub>	80.2	78.0	81.4	80.9	78.9	78.3	80.1	82.5
		AR <sub>50</sub>	89.3	85.8	89.6	88.6	86.3	86.5	88.9	91.0
		$t$ (msec):	10.7	14.4	22.9	34.1	9.5	15.4	23.9	38.0
NVIDIA Jetson AGX Orin 64GB	60W	AP <sub>30-60</sub>	79.6	78.0	80.8	81.2	77.9	77.7	80.7	81.9
		AP <sub>50</sub>	80.2	78.0	81.4	80.9	78.9	78.3	80.1	82.5
		AR <sub>50</sub>	89.3	85.8	89.6	88.6	86.3	86.5	88.9	91.0
		$t$ (msec):	1.6	2.0	3.5	5.3	1.6	2.1	3.9	6.0
AMD Versal SoC VCK190 (INT8)	30W	AP <sub>30-60</sub>	57.6	55.8	50.5	53.1	65.7	54.5	59.8	63.1
		AP <sub>50</sub>	57.6	51.7	45.3	51.6	64.6	50.9	58.0	62.6
		AR <sub>50</sub>	72.4	68.8	69.4	74.2	77.6	72.1	73.2	78.7
		$t$ (msec):	0.24	0.37	0.67	1.0	0.47	0.83	0.83	1.34

**Table 1:** Performance evaluation of YOLOv5 and YOLOv8 models across different devices. AP, AR: average precision, recall (%) at different intersection over union (IoU) thresholds; LATENCY: inference time (milliseconds) for a single image (batch=1); POWER: device power (Watts); <sup>1</sup>half precision (FP16).

These devices encompass diverse processing architectures, from general-purpose processors and GPUs to reprogrammable gate arrays and application-specific tensor processors. The NVIDIA Jetson Nano and Jetson AGX Orin utilize ARM64 CPUs with integrated GPUs (128-core Maxwell for the Nano and 2048-core Ampere for the Orin) to deliver scalable AI performance. The Google Coral Edge TPU features a custom ASIC designed for high-speed, low-power AI inferencing, optimized for TensorFlow Lite models. The AMD Versal SoC combines scalar processors, high-density programmable logic (FPGA), and AI engines targeting vector-based algorithms for real-time DSP and AI computation.

### 4.3. Dataset

We employ a large-scale publicly available image dataset of Mars craters [3], consisting of 102,675 images sourced from a global mosaic [68]. These images are derived from the day-time infrared (DIR) data of the Mars Odyssey Thermal Emission Imaging System (THEMIS) [25], which covers the entire Martian surface with a resolution of 100 meters. Each image measures 25.6 by 25.6 km, translating to 256 x 256 pixels. As illustrated in Figure 2, most craters are small to medium

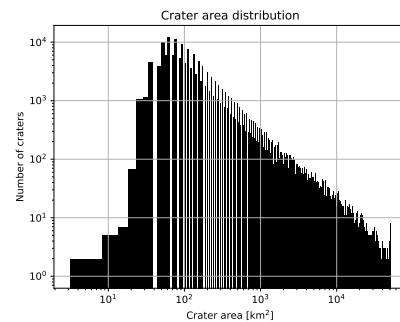


**Figure 2:** Crater Area Distribution from Mars dataset [3]

in size, with the largest craters representing only a small fraction of the total.

### 4.4. Benchmark

In Table 1, we present benchmarking results for YOLOv5 and YOLOv8 models of various sizes, trained on the Mars craters dataset [3] using an NVIDIA V100 Tensor Core GPU. These models were evaluated across eight different devices, measuring Average Precision (AP) and Average Recall (AR) for

detection accuracy, and inference time (t) for latency. Power consumption (in Watts) of each device was also recorded to provide insights into energy efficiency.

IoU thresholds are crucial for craters, which are generally small to medium-sized. Larger objects typically use IoU values above 0.5, indicating substantial overlap between predicted and ground truth bounding boxes. However, smaller objects like craters benefit from lower thresholds due to the higher impact of slight displacements in predictions. Given the predominance of small craters in the dataset (Figure 2), we use metrics with lower IoU thresholds. While maintaining standard AP<sub>50</sub> and AR<sub>50</sub> metrics, AP<sub>30:60</sub> is found to be more indicative compared to AP<sub>50:90</sub>.

#### 4.5. Deployment

Deployment of the models on various architectures requires different approaches based on the underlying hardware and available vendor-specific tools.

For CPUs and the server GPU, deployment was straightforward using our trained PyTorch [69] models without any specific adaptations.

Nvidia Jetson GPUs were employed by using TensorRT [70]. Models were converted from PyTorch to TensorRT engines via ONNX [71], utilizing the YOLO export function provided by ultralytics, to achieve maximum performance.

For the Google Coral Edge TPU, PyTorch models were first converted to ONNX format, then to TensorFlow Lite [72] models, and finally optimized for the Edge TPU using the Edge TPU Compiler [73]. This included quantization to INT8 precision for efficient inference.

Deploying on the Versal SoC VCK190 required significant model adjustments due to unsupported operations. We modified the forward function and post-processing procedures, replaced SiLU [74] layers with LeakyReLU [75], and adjusted the DFL layer to remove unsupported functions. Using Vitis-AI [76], models were quantized to INT8 precision and compiled into DPU subgraphs for execution on Versal.

These varied approaches ensured efficient deployment across all platforms, leveraging each architecture’s specific strengths.

#### 4.6. Results & Discussion

Key factors influencing processing capabilities include the *architecture* of the processing unit, enabling high levels of parallelization, and *hardware efficiency*, enhancing the performance-to-power ratio. For instance, the Edge TPU, a specialized tensor processing unit for machine learning tasks, offers high efficiency and superior performance per watt. For a given architecture, increased power and smaller technology nodes typically improve performance.

Device performance was quantified by measuring inference time for each model on all devices using single

input images (batch size = 1). This approach can overlook other device capabilities, such as increased GPU occupancy/utilization, which could improve data throughput by processing multiple images simultaneously. Quantization on the Edge TPU and Versal SoC affected both recall and precision, converting model weights and activations from 32-bit floating-point numbers to 8-bit fixed-point integers, particularly in post-training quantization (Figure 3).

The Versal SoC showed the highest device performance but considerably lower model accuracy compared to other platforms, attributed to the extensive adjustments required for deployment; however, this can be ameliorated by retraining the model after alteration. Versal SoC achieved the highest processing performance but with relatively increased power consumption, which is a consideration for space avionics.

When including acceleration, the lowest power consumption capabilities were observed on TPU, providing the best performance/Watt in the 5–15W class of devices, comparable even to the Orin GPU built on a more advanced technology node. Edge TPU delivered an order of magnitude faster execution than CPU-based solutions, while the Orin GPU was even faster for larger models due to its larger memory. Overall, the 5–15W embedded devices show remarkable performance-accuracy-power benefits over conventional CPU-based avionics, whereas the 30–60W category enables handling 10–100x more demanding tasks.

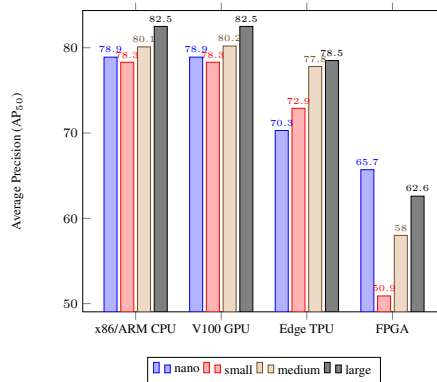


Figure 3: Crater detection AP<sub>50</sub> on Mars dataset [3] for distinct YOLOv8 versions across different architectures

### 5. CONCLUSIONS

We have introduced an approach to real-time crater detection on Mars using YOLO networks for embedded systems. We benchmarked these networks on a large Mars crater dataset across diverse systems. Our results highlight effective trade-offs between power consumption, computational efficiency and performance, demonstrating the feasibility of deploying deep learning networks for autonomous navigation, geological exploration or more.

**Acknowledgements** Simon and Bill were supported by the RAMONES H2020 project (grant: 101017808).

## 6. REFERENCES

- [1] Glenn Jocher, “Ultralytics yolov5,” <https://github.com/ultralytics/yolov5>, 2020. 1, 2, 3
- [2] Glenn Jocher, Ayush Chaurasia, and Jing Qiu, “Ultralytics yolov8,” <https://github.com/ultralytics/ultralytics>, 2023. 1, 2, 3
- [3] Chia-Yu Hsu, Wenwen Li, and Sizhe Wang, “Knowledge-driven geoai: Integrating spatial knowledge into multi-scale deep learning for mars crater detection,” *Remote Sensing*, vol. 13, no. 11, pp. 2116, 2021. 1, 3, 4
- [4] Jean-Baptiste Vincent, Nilda Oklay, Simone Marchi, Sebastian Höfner, and Holger Sierks, “Craters on comets,” *Planetary and Space Science*, vol. 107, pp. 53–63, 2015. 1
- [5] Jean-Pierre Williams, Asmin Pathare, and Oded Aharonson, “The production of small primary craters on mars and the moon,” *Icarus*, vol. 235, pp. 23–36, 06 2014. 1
- [6] Emerson Jacob Speyerer, Reinhold Z. Povilaitis, Mark S. Robinson, Peter C. Thomas, and Robert V. Wagner, “Quantifying crater production and regolith overturn on the moon with temporal imaging,” *Nature*, vol. 538, pp. 215–218, 2016. 1
- [7] Nadine Barlow, “What we know about mars from its impact craters,” *Geological Society of America Bulletin - GEOL SOC AMER BULL*, vol. 122, pp. 644–657, 05 2010. 1
- [8] Robert Craddock, “The origin of phobos and deimos by a giant impact,” pp. 1108–, 10 2011. 1
- [9] Robin Canup, “A giant impact origin of pluto-charon,” *Science (New York, N.Y.)*, vol. 307, pp. 546–50, 02 2005. 1
- [10] William Hartmann and Gerhard Neukum, *Cratering Chronology and the Evolution of Mars*, pp. 165–194, 01 2001. 1
- [11] Neukum B., Boris Ivanov, and W.K. Hartmann, “Cratering records in the inner solar system in relation to the lunar reference system,” 04 2001, vol. 96, pp. 55–86. 1
- [12] G.G. Michael and G. Neukum, “Planetary surface dating from crater size–frequency distribution measurements: Partial resurfacing events and statistical age uncertainty,” *Earth and Planetary Science Letters*, vol. 294, pp. 223–229, 06 2010. 1
- [13] Neukum B., Boris Ivanov, and W.K. Hartmann, “Cratering records in the inner solar system in relation to the lunar reference system,” 04 2001, vol. 96, pp. 55–86. 1
- [14] Nadine Barlow, “Constraining geologic properties and processes through the use of impact craters,” *Geomorphology*, vol. 240, pp. 18–33, 07 2015. 1
- [15] Nadine Barlow, *A review of Martian impact crater ejecta structures and their implications for target properties*, vol. 384, pp. 433–442, 01 2005. 1
- [16] William Hartmann and Stephanie Werner, “Martian cratering 10. progress in use of crater counts to interpret geological processes: Examples from two debris aprons,” *Earth and Planetary Science Letters - EARTH PLANET SCI LETT*, vol. 294, 12 2009. 1
- [17] Ingrid Daubar, C. Atwood-Stone, S. Byrne, A. McEwen, and P. Russell, “The morphology of small fresh craters on mars and the moon,” *Journal of Geophysical Research: Planets*, vol. 119, 12 2014. 1
- [18] Mangold Nicolas, Solmaz Adeli, Susan Conway, Veronique Ansan, and Benoit Langlais, “A chronology of early mars climatic evolution from impact crater degradation,” *Journal of Geophysical Research*, vol. 117, 04 2012. 1
- [19] David Horvath and Jeffrey Andrews-Hanna, “The hydrology and climate of mars during the sedimentary infilling of gale crater,” *Earth and Planetary Science Letters*, vol. 568, pp. 117032, 08 2021. 1
- [20] Yang Cheng, Andrew Johnson, Larry Matthies, and Clark Olson, “Optical landmark detection for spacecraft navigation,” 01 2003, vol. 114. 1
- [21] Chao Zhang, Jinyong Chen, Yanbin Li, Yuqing Li, and Weijie Chai, “Satellite group autonomous operation mechanism and planning algorithm for marine target surveillance,” *Chinese Journal of Aeronautics*, vol. 32, 02 2019. 1
- [22] Diego De Rosa, Ben Bussey, Joshua T. Cahill, Tobias Lutz, Ian A. Crawford, Terence Hackwill, Stephan van Gasselt, Gerhard Neukum, Lars Witte, Andy McGovern, Peter M. Grindrod, and James D. Carpenter, “Characterisation of potential landing sites for the european space agency’s lunar lander project,” *Planetary and Space Science*, vol. 74, no. 1, pp. 224–246, Dec. 2012. 1
- [23] Meng Yu, Hutao Cui, and Yang Tian, “A new approach based on crater detection and matching for visual navigation in planetary landing,” *Advances in Space Research*, vol. 53, no. 12, pp. 1810–1821, 2014. 1

- [24] Stuart Robbins and Brian Hynek, “A new global database of mars impact craters  $\geq 1$  km: 1. database creation, properties, and parameters,” *Journal of Geophysical Research (Planets)*, vol. 117, pp. 5004–, 05 2012. [1](#)
- [25] Philip Christensen, Bruce Jakosky, H. Kieffer, Michael Malin, Harry McSween, Kenneth Neelson, Greg Mehall, Steven Silverman, Steven Ferry, Michael Caplinger, and Michael Ravine, “The thermal emission imaging system (themis) for the mars 2001 odyssey mission,” *Space Science Reviews*, vol. 110, pp. 85–130, 01 2004. [1](#), [3](#)
- [26] James Head, Caleb Fassett, Seth Kadish, David Smith, Maria Zuber, Gregory Neumann, and Erwan Mazarico, “Global distribution of large lunar craters: Implications for resurfacing and impactor populations,” *Science (New York, N.Y.)*, vol. 329, pp. 1504–7, 09 2010. [1](#)
- [27] Stuart J. Robbins, Irene Antonenko, Michelle R. Kirchoff, Clark R. Chapman, Caleb I. Fassett, Robert R. Herrick, Kelsi Singer, Michael Zanetti, Cory Lehan, Di Huang, and Pamela L. Gay, “The variability of crater identification among expert and community crater analysts,” *Icarus*, vol. 234, pp. 109–131, May 2014. [1](#)
- [28] Tara A. Estlin, Rebecca Castaño, Benjamin J. Bornstein, Daniel M. Gaines, Robert C. Anderson, Charles de Granville, David R. Thompson, Michael C. Burl, Michele Judd, and Steve Ankuo Chien, “Automated targeting for the mer rovers,” *2009 Third IEEE International Conference on Space Mission Challenges for Information Technology*, pp. 257–263, 2009. [1](#)
- [29] Richard Castaño, Tara Estlin, Robert Anderson, Daniel Gaines, Andres Castano, Benjamin Bornstein, Caroline Chouinard, and Michele Judd, “Oasis: Onboard autonomous science investigation system for opportunistic rover science,” *J. Field Robotics*, vol. 24, pp. 379–397, 05 2007. [1](#)
- [30] Jung-Rack Kim, J-P Muller, Stephan van Gasselt, Jeremy Morley, and Gerhard Neukum, “Automated crater detection, a new tool for mars cartography and chronology,” *Kim, J.R. and Muller, J.-P. and Van Gasselt, S. and Morley, J.G. and Neukum, G. (2005) Automated crater detection: a new tool for Mars cartography and chronology. Photogrammetric Engineering and Remote Sensing, 71 (10). pp. 1205-1217. ISSN 00991112*, vol. 71, 10 2005. [1](#)
- [31] Y. Sawabe, T. Matsunaga, and S. Rokugawa, “Automated detection and classification of lunar craters using multiple approaches,” *Advances in Space Research*, vol. 37, no. 1, pp. 21–27, 2006. [1](#)
- [32] Lourenço Bandeira, Wei Ding, and Tomasz Stepinski, “Detection of sub-kilometer craters in high resolution planetary images using shape and texture features,” *Advances in Space Research*, vol. 49, pp. 64–74, 01 2012. [1](#)
- [33] Gary Doran, Steven Lu, Maria Liukis, Lukas Mandrake, Umaa Rebbapragada, Kiri Wagstaff, Jimmie Young, Erik Langert, Anneliese Braunegg, Paul Horton, Daniel Jeong, and Asher Trockman, “Cosmic: Content-based onboard summarization to monitor infrequent change,” 03 2020, pp. 1–12. [1](#)
- [34] Svenja Woicke, Andres Moreno Gonzalez, Isabelle El-Hajj, Jelle Mes, Martin Henkel, and Robert Klavers, “Comparison of crater-detection algorithms for terrain-relative navigation,” 01 2018. [1](#)
- [35] Nur Diyana Kamarudin, Kamaruddin Abd. Ghani, Mu-hazam Mustapha, Ariffin Ismail, and Nik Ghazali Nik Daud, “An overview of crater analyses, tests and various methods of crater detection algorithm,” 2014. [1](#)
- [36] Jihao Yin, Yin Xu, Hui Li, and Yueshan Liu, “A novel method of crater detection on digital elevation models,” in *2013 IEEE International Geoscience and Remote Sensing Symposium - IGARSS*, 2013, pp. 2509–2512. [1](#)
- [37] Goran Salamunićcar, Sven Lončarić, and Erwan Mazarico, “Lu60645gt and ma132843gt catalogues of lunar and martian impact craters developed using a crater shape-based interpolation crater detection algorithm for topography data,” *Planetary and Space Science*, vol. 60, no. 1, pp. 236–247, 2012. [1](#)
- [38] Danielle DeLatte, Sarah Crites, Nicholas Guttenberg, Elizabeth Tasker, and Takehisa Yairi, “Segmentation convolutional neural networks for automatic crater detection on mars,” *IEEE Journal of Selected Topics in Applied Earth Observations and Remote Sensing*, vol. PP, pp. 1–14, 06 2019. [1](#), [2](#)
- [39] Yanmin Jin, Fan He, Shijie Liu, and Xiaohua Tong, “Small scale crater detection based on deep learning with multi-temporal samples of high-resolution images,” 08 2019, pp. 1–4. [1](#), [2](#)
- [40] Atal Tewari, K Prateek, Amrita Singh, and Nitin Khanna, “Deep learning based systems for crater detection: A review,” *arXiv preprint arXiv:2310.07727*, 2023. [1](#)
- [41] Kirsten Weide-Zaage, Guillermo Paya-Vaya, Katharina Schmidt, and Dorian Hagenah, “Investigation of fpga and sram cells under radiation exposure,” in *2022 23rd International Conference on Thermal, Mechanical and*

*Multi-Physics Simulation and Experiments in Microelectronics and Microsystems (EuroSimE)*, 2022, pp. 1–5. 1

- [42] Alexander Huber, Gennady Sergienko, David Kinna, Valentina Huber, Alberto Milocco, Laurent Mercadier, Itziar Balboa, Sean Conroy, Simon Cramp, Vasili Kiptily, Uron Kruezi, Horst Toni Lambertz, Christian Linsmeier, Guy Matthews, Sergey Popovichev, Philippe Mertens, Scott Silburn, and Klaus-Dieter Zastrow, “Response of the imaging cameras to hard radiation during jet operation,” *Fusion Engineering and Design*, vol. 123, pp. 669–673, 2017, Proceedings of the 29th Symposium on Fusion Technology (SOFT-29) Prague, Czech Republic, September 5-9, 2016. 1
- [43] Joseph Redmon, Santosh Divvala, Ross Girshick, and Ali Farhadi, “You only look once: Unified, real-time object detection,” in *Proceedings of the IEEE conference on computer vision and pattern recognition*, 2016, pp. 779–788. 1
- [44] Alexey Bochkovskiy, Chien-Yao Wang, and Hong-Yuan Mark Liao, “Yolov4: Optimal speed and accuracy of object detection,” *arXiv preprint arXiv:2004.10934*, 2020. 1
- [45] Crater Group, Raymond Arvidson, J. Boyce, C. Chapman, Mark Cintala, M. Fulchignoni, H. Moore, G. Neukum, P. Schultz, L. Soderblom, R. Strom, Alex Woronow, and R. Young, “Standard techniques for presentation and analysis of crater size-frequency data,” *Icarus*, vol. 37, pp. 467–474, 01 1979. 2
- [46] Osamu Konishi, Ryushi Azuma, Hisashi Yokogawa, Syuta Yamanaka, and Yuichi Iijima, “Data mining system for planetary images - crater detection and categorization -,” 07 2000. 2
- [47] M. C. Burl, T. Stough, W. Colwell, E. B. Bierhaus, W. J. Merline, and C. Chapman, “Automated detection of craters and other geological features,” 2001. 2
- [48] Teresa Barata, Eduardo Alves, José Saraiva, and Pedro Pina, “Automatic recognition of impact craters on the surface of mars,” 10 2004, vol. 3212, pp. 489–496. 2
- [49] Erik Urbach and Tomasz Stepinski, “Automatic detection of sub-km craters in high resolution planetary images,” *Planetary and Space Science*, vol. 57, pp. 880–887, 06 2009. 2
- [50] Danielle DeLatte, S.T. Crites, N. Guttenberg, and T. Yairi, “Automated crater detection algorithms from a machine learning perspective in the convolutional neural network era,” *Advances in Space Research*, vol. 64, 07 2019. 2
- [51] Ari Silburt, Mohamad Ali-Dib, Chenchong Zhu, Alan Jackson, Diana Valencia, Yevgeni Kissin, Daniel Tamayo, and Kristen Menou, “Lunar crater identification via deep learning,” *Icarus*, vol. 317, 03 2018. 2
- [52] P. Naidoo and M. Sibanda, *Embedded Supercomputing for Edge Devices: A Comprehensive Review*, pp. 157–173, Springer Nature Switzerland, Cham, 2024. 2
- [53] Asier Garcia-Perez, Raúl Miñón, Ana I. Torre-Bastida, and Ekaitz Zulueta-Guerrero, “Analysing edge computing devices for the deployment of embedded ai,” *Sensors*, vol. 23, no. 23, 2023. 2
- [54] Herbert Woisetschläger, Alexander Isenko, Ruben Mayer, and Hans-Arno Jacobsen, “Fledge: Benchmarking federated machine learning applications in edge computing systems,” 2023. 2
- [55] George Lentaris, Konstantinos Maragos, Ioannis Stratakos, Lazaros Papadopoulos, Odysseas Papanikolaou, Dimitrios Soudris, Manolis Lourakis, Xenophon Zabulis, David Gonzalez-Arjona, and Gianluca Furano, “High-performance embedded computing in space: Evaluation of platforms for vision-based navigation,” *Journal of Aerospace Information Systems*, vol. 15, no. 4, pp. 178–192, 2018. 2
- [56] Gianluca Furano, Gabriele Meoni, Aubrey Dunne, David Moloney, Veronique Ferlet-Cavrois, Antonis Tavoularis, Jonathan Byrne, Léonie Buckley, Mihalis Psarakis, Kay-Obbe Voss, and Luca Fanucci, “Towards the use of artificial intelligence on the edge in space systems: Challenges and opportunities,” *IEEE Aerospace and Electronic Systems Magazine*, vol. 35, no. 12, pp. 44–56, 2020. 2
- [57] Kiruki Cosmas and Asami Kenichi, “Utilization of fpga for onboard inference of landmark localization in cnn-based spacecraft pose estimation,” *Aerospace*, vol. 7, no. 11, 2020. 2
- [58] Glenn Jocher, Ayush Chaurasia, and Jing Qiu, “Ultralytics YOLO,” <https://github.com/ultralytics/ultralytics>, Jan. 2023. 2
- [59] Chien-Yao Wang, Hong-Yuan Mark Liao, Yueh-Hua Wu, Ping-Yang Chen, Jun-Wei Hsieh, and I-Hau Yeh, “Cspnet: A new backbone that can enhance learning capability of cnn,” in *Proceedings of the IEEE/CVF conference on computer vision and pattern recognition workshops*, 2020, pp. 390–391. 2
- [60] Kaiming He, Xiangyu Zhang, Shaoqing Ren, and Jian Sun, “Spatial pyramid pooling in deep convolutional networks for visual recognition,” *IEEE transactions on pattern analysis and machine intelligence*, vol. 37, no. 9, pp. 1904–1916, 2015. 2

- [61] Shu Liu, Lu Qi, Haifang Qin, Jianping Shi, and Jiaya Jia, "Path aggregation network for instance segmentation," in *Proceedings of the IEEE conference on computer vision and pattern recognition*, 2018, pp. 8759–8768. 2
- [62] NVIDIA Corporation, "Nvidia jetson nano developer kit (4gb)," <https://developer.nvidia.com/embedded/jetson-nano-developer-kit>, 2020, Accessed: 2024-05-25. 2
- [63] NVIDIA Corporation, "Nvidia jetson agx orin developer kit (64gb)," <https://developer.nvidia.com/embedded/jetson-agx-orin-developer-kit>, 2022, Accessed: 2024-05-25. 2
- [64] Google, "Google coral edge tpu development kit (1gb)," <https://coral.ai/products/dev-board/>, 2019, Accessed: 2024-05-25. 2
- [65] AMD, "Amd fpga soc vck190 evaluation kit," <https://www.xilinx.com/products/boards-and-kits/vck190.html>, 2021, Accessed: 2024-05-25. 2
- [66] Intel Corporation, "Intel xeon gold 5218r processor," <https://www.intel.com/content/www/us/en/products/details/processors/xeon/scalable/gold.html>, 2020, Accessed: 2024-05-25. 2
- [67] NVIDIA Corporation, "Nvidia v100 tensor core gpu," <https://www.nvidia.com/en-us/data-center/v100/>, 2017, Accessed: 2024-05-25. 2
- [68] Christopher Edwards, Keith Nowicki, P. Christensen, J. Hill, N. Gorelick, and K. Murray, "Mosaicking of global planetary image datasets: 1. techniques and data processing for thermal emission imaging system (themis) multi-spectral data," *Journal of Geophysical Research*, vol. 116, 10 2011. 3
- [69] Adam Paszke, Sam Gross, Soumith Chintala, Gregory Chanan, Edward Yang, Zachary DeVito, Zeming Lin, Alban Desmaison, Luca Antiga, and Adam Lerer, "Automatic differentiation in pytorch," 2017. 4
- [70] NVIDIA, "Nvidia tensorrt," <https://developer.nvidia.com/tensorrt>, 2024, Accessed: 2024-05-25. 4
- [71] Junjie Bai, Fang Lu, Ke Zhang, et al., "Onnx: Open neural network exchange," <https://github.com/onnx/onnx>, 2019. 4
- [72] TensorFlow, "Tensorflow lite," <https://www.tensorflow.org/lite>, 2024, Accessed: 2024-05-25. 4
- [73] Coral, "Edge tpu compiler," <https://coral.ai/docs/edgetpu/compiler/>, 2024, Accessed: 2024-05-25. 4
- [74] Stefan Elfving, Eiji Uchibe, and Kenji Doya, "Sigmoid-weighted linear units for neural network function approximation in reinforcement learning," *Neural networks*, vol. 107, pp. 3–11, 2018. 4
- [75] Bing Xu, Naiyan Wang, Tianqi Chen, and Mu Li, "Empirical evaluation of rectified activations in convolutional network," *arXiv preprint arXiv:1505.00853*, 2015. 4
- [76] Xilinx, "Vitis ai," <https://www.xilinx.com/products/design-tools/vitis/vitis-ai.html>, 2024, Accessed: 2024-05-25. 4